

Motion Planning and Compliant Control for a Quadruped Robot on Complicated Terrains

Xuesong Shao*, Qifeng Huang, Zhongdong Wang, and
Qixin Cai

*State Grid Jiangsu Electric Power Research Institute
State Grid Key Laboratory of Electric Energy Measurement
Nanjing, Jiangsu Province, China*

xuesong.shao@gmail.com, hqfyqhgy@126.com,
wzd_jsepc@sina.com, cqx6503@163.com

Wei Wang

*Institute of Automation
Chinese Academy of Sciences
Beijing, 100190, China*

wei.wang@ia.ac.cn

Abstract - Quadruped robots have the superiority to locomote on complicated terrains. However, in unknown environments, adaptive locomotion is still a great challenge. Considering the terrains including convex obstacles and forbidden areas, a novel motion planning algorithm is investigated for path planning, gait generation, gait transition and foothold searching. According to the terrain maps built by on-board stereo vision, the quadruped robot chooses the suitable gaits independently. Walk gait is selected on unstructured road segments for more stability while trot gait is employed on flat ground for higher speed. The motion trajectories are performed in the low level compliant control based on the kinematics and the couple dynamics which depends on stance phase and swing phase. The emphases of our inverse dynamics model are the analyses of the couple influences between four legs and the transition between different motion stages. The control architecture is applied on a real quadruped robot, and the experiment results demonstrate the availability of the system.

Index Terms - Quadruped robot; Motion planning; Inverse dynamics; Gait control

I. INTRODUCTION

In recent years, many researchers have realized that compared to wheeled robots, legged robots have superiorities of locomotion on unstructured complicated terrains because of their maneuverability and flexibility. As a kind of typical legged robots, quadruped robots which have higher stability and efficiency are being widely studied. TITAN robots, designed by Hirose et al. since the 1980s, could deal with some discontinuous terrains, such as stairs, slopes, and rugged environments [1][2]. Kimura et al. developed Tekken and Kotetsu robots, which were mainly controlled by Central Pattern Generator (CPG). Some experiments were performed on natural ground about dynamic walking [3]-[6]. SCOUT II, which has only one actuated revolute joint on each leg, was used to perform bound gait at a relatively high speed [7]. As a research platform for educational institutions, the reptilian quadruped robot SILO6 could be implemented with static gaits[8]. The famous quadruped robot BigDog, designed and built by Boston Dynamics, showed good performance with dynamic stability. Because of the robust mechanical structure and the effective control algorithm, it even had the ability of walking on terrains with ice or snow [9]-[11]. The above

quadruped robots performed well in certain situations with complicated terrains.

In practical application, environments may be different and terrains may always change. How to walk adaptively in unknown environments becomes a challenge task for quadruped locomotion. In this paper, we present the control system for locomotion autonomously in unknown complicated ground. The upper part of the whole control architecture is environment modeling through stereo vision sensing, which has been discussed in our previous research [12]. The grid terrain model is built for motion planning with attitude angles calculated from the gyroscope. In the environments, there are convex obstacles and forbidden areas scattering on the ground. Considering the features of the terrains, the motion planning algorithm which contains multiple gait generation and gait transition chooses waypoints for generating smooth foot trajectories. This can improve the locomotion performance through trotting on continuous road segments fast and walking on discontinuous road segments steadily. The low level makes use of the compliant control method. With the effective forward/inverse kinematics models and the couple inverse dynamics model, the compliant control algorithm is given.

The rest of the paper is organized as follows. Section II presents the motion planning algorithm and Section III discusses the low level compliant control. The experiments are carried out and analyzed in Section IV. Finally, Section V concludes the paper and suggests the future work.

II. MOTION PLANNING ALGORITHM

To cross over unknown complicated terrain, the motion planner in the control system must evaluate the terrain and present the most suitable footholds to the quadruped robot's low level controller. There are some key factors that should be considered, stability, flexibility, and locomotion speed. In the quadruped robot locomotion, stability is the basic requirement for successful walking without tumbling and sliding. Flexibility can be described as the quadruped robot's foot trajectories should be smooth while traversing [13]. The reason of choosing the walking speed as a factor is that the quadruped robot should not only negotiate the challenging terrain successfully but also as fast as possible.

In order to evaluate the terrain, the cost map is generated

according to terrain's grid map. Firstly, the grid cells of forbidden regions, cost values of which are considered as infinity, are sorted out. Besides, for the sake of stability while walking, the height of each remaining cell and its change rate are taken into consideration. For the grid cell at the i th row and the j th column, the cost value is denoted by $Cost_{ij}$ and can be formulated as

$$Cost_{ij} = h_{ij} + Dev(h_{ij}), \quad (1)$$

where, h_{ij} is the height of the cell, $Dev(h_{ij})$ describes the cell's change to elements in 3×3 neighborhood with the following form,

$$Dev(h_{ij}) = \frac{|h_{ij} - h_{(i-1)j}|}{2} + \frac{|h_{ij} - h_{i(j-1)}|}{2} + \frac{|h_{ij} - h_{i(j+1)}|}{2} + \frac{|h_{ij} - h_{(i+1)j}|}{2} + \frac{|h_{ij} - h_{i(j-1)}|}{2\sqrt{2}} + \frac{|h_{ij} - h_{(i-1)(j+1)}|}{2\sqrt{2}} + \frac{|h_{ij} - h_{(i+1)(j-1)}|}{2\sqrt{2}} + \frac{|h_{ij} - h_{(i+1)(j+1)}|}{2\sqrt{2}}, \quad (2)$$

where, $h_{(i-1)(j-1)}$, $h_{(i-1)j}$, $h_{(i-1)(j+1)}$, $h_{i(j-1)}$, h_{ij} , $h_{i(j+1)}$, $h_{(i+1)(j-1)}$, $h_{(i+1)j}$, $h_{(i+1)(j+1)}$ stand for the heights of elements in the 3×3 neighborhood of the cell.

Another key factor is the quadruped robot walking speed. Generally, to improve the walking efficiency, the measure which is easily conceived is increasing the joint motors' rotating velocity. However, for some big quadruped robots, they have large weight because of the materials and load is usually added on them, so the joint motors almost work at full capacity. In our motion planning algorithm, multiple typical gaits and gait transition strategy are employed. Through gait transition, the most efficient movement with both minimum energy consumption and maximal stability is selected. Trot gait which has higher speed is adopted to locomote on the road sections without obstacles, while in unstructured road conditions, for maintaining the stability, walk gait is utilized to improve the maneuverability. Furthermore, the moving distance of the body in each period is settled. In this way, the quadruped robot can cross over complicated terrains with both considerable safety and velocity.

Considering the development of motion strategy in anterior and posterior directions, search areas in foot coordinate systems are fixed with X coordinates equaling to zero. The key elements in the motion planning algorithm are listed as

- 1) Determine the search range for each step.
- 2) Deal with the forbidden areas in the search range.
- 3) Determine which point is the most suitable foothold.
- 4) Avoid the foothold trapped in some minimal cell.

To solve those problems, the planning process is carried out in

each foot coordinate system and current search ranges are determined according to the search results of former steps. The formal description of the motion planning algorithm is given in Fig. 1. Search areas are computed for finding optimal footholds. If a cost value in search area is less than the threshold value, the position is nearly located on flat ground plane. The quadruped robot changes locomotion manners and adjusts gait generation strategies according to the conditions of grid terrain maps. The first step is to decide whether there are forbidden areas in current search areas. When no forbidden region exists, any point in search areas may be the potential foothold. When all of the values in search areas for four legs are less than the threshold value, if four feet are in proper positions, then trot gait is selected for the next moving period, otherwise walk gait is chosen with each stride equaling to half of the search distance. When convex obstacles are detected in the walking path, to avoid selecting the foothold at the position with local minimum value, large weights are assigned to the cost values of the positions at the boundaries of search areas. On the contrary, to avoid the forbidden regions, walk gait is selected and the search areas are divided into some sub areas. Similarly, if there are no convex obstacles in all of the sub search areas, the foothold is selected at the nearest point to the median value of the search range for a proper walking stride, otherwise the foothold is chosen at the minimum cost value and a weight larger than 1, for example 1.1, is assigned to the value. What's more, to maintain the stability while moving with walk gait, a posture adjustment strategy based on potential energy is utilized through changing lengths of legs in diagonal to put the center of gravity (COG) into the support polygon [13].

III. COMPLIANT CONTROL

The motion planning algorithm chooses the waypoints which four feet should follow on complicated terrains. In this section, to control the robot to achieve the motion accurately, we build the forward/inverse kinematics models and inverse dynamics model, and design the low level compliant control algorithm.

A. The kinematics

The quadruped robot is a complicated multi-body mechanical system composed of several links and joints. It is necessary to build the data structure for the quadruped modeling and programming. Through referring to the humanoid robot data structure construction method proposed by Kajita *et al.* [14], our robot organization relationship is constructed as Fig. 2. RF, LH, LF, and RH stand for right front, left hind, left front, and right hind respectively. Each link has two branches, which are the child link on the left side and the sister link on the right side. In addition, except the body, each link has one joint. Therefore, the same modeling algorithm is applicable to all the rod/joint pairs and it is convenient for recursive programming.

Algorithm Motion Planning (${}^kL_0, {}^wL_0, A, {}^kC, {}^kG, {}^kL_{\max}, Threshold$)

Parameters:

$k = RF, RH, LF, LH$

kL_0 : initial foot position at the beginning to foot coordinate system

wL_0 : initial position of the projection of the center of quadruped body to world coordinate system

A : body movement during each period

kC : cost map in foot coordinate system

kG : grid map in foot coordinate system

${}^kL_{\max}$: maximum planning distance

$Threshold$: threshold value for comparison with values in cost map

For $i = 1, \dots, n$

For $k = RF, \dots, LH$

Define ${}^k s_i, {}^k D_i, {}^k L_i, {}^w L_i$

${}^k s_i$: stride in the i th step

${}^k D_i$: search area in the i th step

${}^k L_i$: foot position to foot coordinate system after the i th step

${}^w L_i$: position of the projection of the center of quadruped body to world coordinate system after the i th step

${}^k D_i = [{}^k L_{i-1}, {}^w L_{i-1} + 2A]$

For $k = RF, \dots, LH$

If no forbidden areas in ${}^{RF}D_i, {}^{RH}D_i, {}^{LF}D_i, {}^{LH}D_i$

If each of the cost values in ${}^{RF}D_i, {}^{RH}D_i, {}^{LF}D_i, {}^{LH}D_i$ less than $Threshold$

If ${}^k L_{i-1} - {}^w L_{i-1} < A/2, (k = RF, \dots, LH)$

Select trot gait, ${}^k s_i = A$

Else

Select walk gait, ${}^k s_i = (2A + {}^w L_{i-1} - {}^k L_{i-1})/2$

Else

Select walk gait

Assign different weights to cost value according to

$\omega = \left(x - {}^k L_{i-1} - \frac{{}^w L_{i-1} + 2A - {}^k L_{i-1}}{2} \right)^2 + A,$

$x \in {}^k D_i$

Find foothold at minimum cost value in ${}^k D_i$

Else

Select walk gait

Find forbidden areas, $[{}^k B_{11}, {}^k B_{12}], \dots, [{}^k B_{j1}, {}^k B_{j2}]$, where j is the number of forbidden areas

Determine sub search areas, $[{}^k L_{i-1}, {}^k B_{11}], \dots, [{}^k B_{(j-1)2}, {}^k B_{j1}], [{}^k B_{j2}, {}^w L_{i-1} + 2A]$

If each of the cost values in sub search areas less than $Threshold$

Select the nearest point to median value

$(2A + {}^w L_{i-1} - {}^k L_{i-1})/2$

Else

Find foothold at minimum cost value in ${}^k D_i$

Assign weight $\omega = 1.1$ to the cell

${}^k L_i = {}^k L_{i-1} + {}^k s_i$

${}^w L_i = {}^w L_{i-1} + A$

Select waypoints according to the mixed parabola method

If ${}^k L_i \geq {}^k L_{\max}$

Return.

Fig. 1 Motion planning algorithm for moving forwards and backwards, containing gait generation, gait transition and foothold searching.

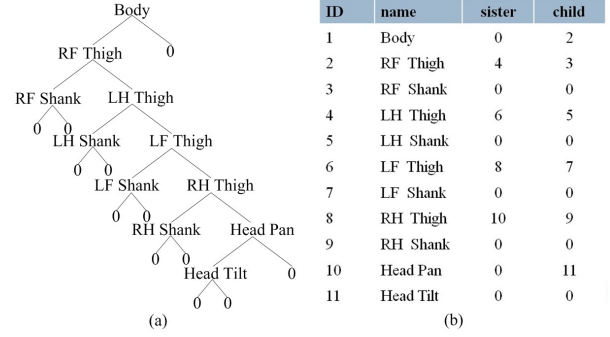


Fig. 2 The quadruped organization relationship. Each link has one child link and one sister link in the data structure and zero indicates there is no sub-link.

Due to the simplicity and flexibility, as well as the accuracy during coordinate transformation, the Rodrigues rotation formula is more suitable in the robot's forward kinematics modeling [15]. The Rodrigues rotation formula which defines the rotation matrix can be expressed as

$$e^{(\mathbf{a} \times 1)\theta} = \mathbf{I} + (\mathbf{a} \times 1)\sin \theta + (\mathbf{a} \times 1)^2(1 - \cos \theta), \quad (3)$$

where, $\mathbf{I} \in \mathbf{R}^{3 \times 3}$ is the identity matrix, θ is the joint angle and $\mathbf{a} \in \mathbf{R}^{3 \times 1}$ is the joint axis vector, which is the unit vector of the joint velocity $\boldsymbol{\omega} = [\omega_x, \omega_y, \omega_z]^T$ and can be expressed as $\boldsymbol{\omega} = \mathbf{a} \omega$. Also the description of $\boldsymbol{\omega} \times 1$ is given by

$$\boldsymbol{\omega} \times 1 = \begin{bmatrix} 0 & -\omega_z & \omega_y \\ \omega_z & 0 & -\omega_x \\ -\omega_y & \omega_x & 0 \end{bmatrix}. \quad (4)$$

To convert waypoints from task space into joint space for joint motion, inverse kinematics must be considered. Usually, the analytical method or the geometric method is used for the inverse calculation. Through solving the matrix equation of forward kinematics, the corresponding joint angles can be obtained. However, because of operation of matrix inversion, the cases of multiple solutions and no solution may occur. So we employ numerical method to find the approximate joint angles for inverse kinematics solution here. The basic idea is successive approximation through forward kinematics calculating repeatedly. As in Fig. 3, with the given initial joint angles, current pose can be computed. Then, by analyzing the error between target pose and current pose, the correction values of joint angles come out. Among them, two key elements should be considered seriously. One is the loop termination condition and the other is the calculation of the correction value. As to the first problem, we can evaluate the error by the following equation,

$$error = \alpha \|\mathbf{p}_{\text{tar}} - \mathbf{p}_{\text{cur}}\|^2 + \beta \|\boldsymbol{\omega}_{\text{tar}} - \boldsymbol{\omega}_{\text{cur}}\|^2, \quad (5)$$

where, \mathbf{p}_{tar} is the target position vector, \mathbf{p}_{cur} is the current position vector, $\boldsymbol{\omega}_{\text{tar}}$ is the target angular velocity vector, and $\boldsymbol{\omega}_{\text{cur}}$ is the current angular velocity vector, α and β are scale coefficients. If the error is less than a minimum value, for example, $1e-6$, or the iteration times comes up to the upper limit, the solving process would stop and the current joint angles are the final inverse kinematics solution results.

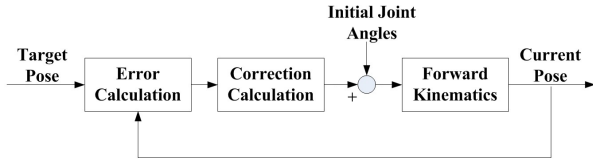


Fig. 3 The inverse kinematics solving process. The final joint angles come from the iterative computation of the forward kinematics.

The correction value utilizes the Jacobian matrix \mathbf{J} which reveals the relationship between the joint velocity and the terminal velocity. The joint correction value $\Delta\theta$ can be approximately calculated as

$$\Delta\theta = \lambda \mathbf{J}^{-1} [\Delta\mathbf{p}, \Delta\boldsymbol{\omega}]^T, \quad (6)$$

where, $[\Delta\mathbf{p}, \Delta\boldsymbol{\omega}]^T = [\mathbf{p}_{\text{tar}} - \mathbf{p}_{\text{cur}}, \boldsymbol{\omega}_{\text{tar}} - \boldsymbol{\omega}_{\text{cur}}]^T$ is the pose error, and λ is the adjustment coefficient. The final corresponding joint angles are interpolated using cubic spline interpolation method. In order to prevent discontinuous change between different steps, all of the joint position values are considered as a whole for interpolation.

B. The couple inverse dynamics controller

To achieve the fast and high-precision quadruped locomotion, inverse dynamics should be resolved to get the joint torques with the joint angles, velocities, and accelerations. For robots with floating bases, such as humanoid robots, quadruped robots, and so on, the traditional inverse dynamics methods are based on the virtual 6-DOF joint, which is added manually to connect the floating base to a fixed point in world coordinate system [16]-[19]. These methods are easy to understand but complicated to calculate because of the virtual joint. Referring to the characteristics of quadruped motion, an inverse dynamics modeling method is developed based on the legs' stance phase and swing phase [15]. The quadruped robot is divided into four independent leg serial linkages. For each leg serial linkage, different fixed bases are set according to the different motion stages. When a leg is in stance phase, the knee joint is regarded as the fixed base frame for the leg serial linkage; otherwise the hip joint is set as the fixed base frame. So, the inverse dynamics equations are expediently constructed with lower computational complexity. However, this dynamics model skips that the four legs of the quadruped robot is an

interrelated entity and one leg's motion would generate influence to the other three legs. Again, for each leg, there is no transition stage between the different inverse dynamics models in both stance phase and swing phase. Jerking motion would occur from one stance to the other.

To uncover the kinetic laws, the couple dynamics model is built for the quadruped robot based on stance phase and swing phase, which focuses on the influences between four legs and the transition between two phases. Each of the four leg serial linkages includes one of the four legs. As they have similar configuration to each other, we take one of them to get insight on the inverse dynamics models.

When the leg is in stance phase, the shank is supposed to be the base and the origin coincides with the knee joint. The hip joint takes care of the body's movement and forces acting on the body, including gravity and the other three hip joints' action. The knee joint compensates for the thigh's gravity and hip joint's action, and deals with the thigh's movement. The inverse dynamics can be iteratively computed from the body to the shank by the following equations,

$$\begin{bmatrix} f_{ih} \\ \tau_{ih} \end{bmatrix} + \begin{bmatrix} f_{ib}^g \\ \tau_{ib}^g \end{bmatrix} - \sum_{j \neq i} \omega_{ij} \begin{bmatrix} f_{jh} \\ \tau_{jh} \end{bmatrix} = I_b^S \dot{\xi}_{ib} + \xi_{ib} \times I_b^S \xi_{ib}, \quad (7)$$

$$\begin{bmatrix} f_{ik} \\ \tau_{ik} \end{bmatrix} + \begin{bmatrix} f_{it}^g \\ \tau_{it}^g \end{bmatrix} - \begin{bmatrix} f_{ih} \\ \tau_{ih} \end{bmatrix} = I_t^S \dot{\xi}_{it} + \xi_{it} \times I_t^S \xi_{it}. \quad (8)$$

The parameters here and others from (9)-(12) are illustrated in detail in Tab. 1. When the leg is in swing phase, the body is considered as the base and the origin is in accord with the hip joint. The knee joint takes care of the shank's movement and gravity. The hip joint not only deals with the thigh's gravity, knee joint's action, and other three hip joints' actions but also responds to the thigh's movement. From the shank to the body, the inverse dynamics in swing phase can be iteratively calculated as

$$\begin{bmatrix} f_{ik} \\ \tau_{ik} \end{bmatrix} + \begin{bmatrix} f_{is}^g \\ \tau_{is}^g \end{bmatrix} = I_s^S \dot{\xi}_{is} + \xi_{is} \times I_s^S \xi_{is}, \quad (9)$$

$$\begin{bmatrix} f_{ih} \\ \tau_{ih} \end{bmatrix} + \begin{bmatrix} f_{it}^g \\ \tau_{it}^g \end{bmatrix} - \begin{bmatrix} f_{ik} \\ \tau_{ik} \end{bmatrix} - \sum_{j \neq i} \omega_{ij} \begin{bmatrix} f_{jh} \\ \tau_{jh} \end{bmatrix} = I_t^S \dot{\xi}_{it} + \xi_{it} \times I_t^S \xi_{it}. \quad (10)$$

With the forces and torques above, the actuator torques on the axes of hip joint and knee joint can be given as

$$u_{ih} = [p_{ih} \times a_{ih}] \begin{bmatrix} f_{ih} \\ \tau_{ih} \end{bmatrix}, \quad (11)$$

$$u_{ik} = [p_{ik} \times a_{ik}] \begin{bmatrix} f_{ik} \\ \tau_{ik} \end{bmatrix}. \quad (12)$$

The couple dynamics model includes transition stages to avoid jerking motion while phases switching. The transition period t_s between different kinds of phases, which can be adjusted flexibility according to the length of phases, should be firstly

decided. The actuator torques increase or decrease linearly in the transition stage. The transfer function can be described as

$$U = \begin{cases} fU_{stance} + (1-f)U_{swing} & |t| < t_s \\ F_{stance}U_{stance} + F_{swing}U_{swing} & \text{else} \end{cases}, \quad (13)$$

where, t is the time, U_{stance} and U_{swing} are the actuator torque vectors in stance phase and swing phase respectively, F_{stance} and F_{swing} are sign flags, for example, $F_{stance} = 1, F_{swing} = 0$ in stance phase, $f = -t/2t_s + 1/2$ while switching from stance phase to swing phase, otherwise $f = t/2t_s + 1/2$.

TABLE I
PARAMETERS DESCRIPTION FOR THE COUPLE INVERSE DYNAMICS

	Description
i, j	$i, j = \text{RF, LH, LF, RH, and } i \neq j$
f_{ih}, f_{jh}	forces of the i th and the j th hip joints
f_{ik}	force of the i th knee joint
$f_{ib}^g, f_{it}^g, f_{is}^g$	gravities of the i th body, thigh and shank
τ_{ih}, τ_{jh}	torques of the i th and the j th hip joints
τ_{ik}	torque of the i th knee joint
$\tau_{ib}^g, \tau_{it}^g, \tau_{is}^g$	gravitational torques of the i th body, thigh and shank
u_{ih}, u_{ik}	actuator torques of the i th hip and knee joints
p_{ih}, p_{ik}	position vectors of the i th hip and knee joints
a_{ih}, a_{ik}	joint axis vectors of the i th hip and knee joints
I_b^s, I_t^s, I_s^s	spatial inertial tensors of the body, thigh and shank
$\dot{\xi}_{ib}, \dot{\xi}_{it}, \dot{\xi}_{is}$	6D spatial velocity vectors of the i th body, thigh and shank
$\ddot{\xi}_{ib}, \ddot{\xi}_{it}, \ddot{\xi}_{is}$	6D spatial acceleration vectors of the i th body, thigh and shank
ω_{ij}	weight of the j th hip joint to the i th hip joint, $\omega_{ij} = \pm 1$

In the inverse dynamics model, the quadruped robot is considered as an indivisible entity through adding coupling factors. One leg's motion would generate the force to the rest legs. In the calculation of the inverse dynamics algorithm, the coupling forces and torques from other serial robots can be replaced approximately by the values of previous time. The initial values of forces and torques are supposed to be zeros. Then, the solution of the couple inverse dynamics model can veritably reveal the quadruped robot's dynamic characteristics.

On unstructured complicated terrains, the motion trajectories may deviate from desired positions compared to periodic locomotion on flat roads [20]. Fig. 4 describes the compliant torque control method, which is implemented for the low level control to avoid the motion deviation and realize compliant locomotion. The control scheme includes a feed-back PD controller and an inverse dynamics feed-forward controller. Based on the inverse kinematics, the waypoints

coming from motion planning algorithm in task space are transformed into joint angles. The sum of the feed-forward torque u_{ff} and the output of the PD controller u_{fb} is taken as the input torque u to the quadruped robot.

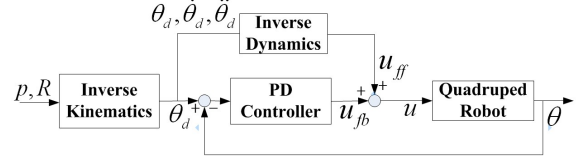


Fig. 4 The diagram of the couple inverse dynamics control. The control torque comes from both the PD controller and the feed-forward inverse dynamics controller.

IV. EXPERIMENTS

A. Locomotion on complicated terrains

The experiments are carried out in indoor environment with smooth floor, which is textureless and reflective under the irradiation of fluorescent lamps. Stone blocks, which scatter on the floor randomly, are selected with the maximum size of about $0.15m \times 0.15m \times 0.2m$. Forbidden areas on the floor are indicated as the regions covered with black carpets for convenience. To get accurate terrain models, the camera with the resolution of 640×480 is set to sense the terrains within two meters. The experiments based on the three kinds of terrains, which are the convex obstacle terrain, the forbidden area terrain and the mixed terrain with both convex obstacles and forbidden areas respectively, are conducted to verify the effectiveness of our adaptive locomotion system.

The control architecture is implemented on the quadruped robot FROG, built at our lab, shown in Fig. 5. FROG is about 1.15m long, 0.7m wide, and 0.95m tall, with a total weight of approximately 55kg. Each leg has one hip pitch joint and one knee pitch joint, both of which are powered by DC motors. Still, each toe possesses one passive compliant prismatic DOF which can be used to detect the contact between the foot and the ground [13] [21] [22]. The stereo camera is mounted on the pan/tilt platform, and the gyroscope is placed at the center of the quadruped body to sense the attitude. An embedded controller performs actuator control and communicates with vision process computer.

In adaptive locomotion, the camera's blind area between the quadruped robot itself and the nearest positions of the perception terrains can be modeled as flat ground planes, supposing that there are no convex obstacles or forbidden areas. In order to walk more smoothly, the distance of body movement during each period is set to 0.2m from a lot of experiments. According to the terrain modeling errors, the variable of height *Threshold* is set to 0.02m, that is, any grid cell with the height below 0.02m can be considered as flat ground plane area. The initial positions of kL_0 and wL_0 can be calculated with the initial joint angles. Fig. 6 displays the snapshots of locomotion with stereo vision on complicated

terrains for FROG. The moving sequence in each subpicture is top left, top right, bottom left, and bottom right. In a walk period, the legs' moving sequence is RF-LH-RH-LF. RF and LH legs move simultaneously before LF and RH in a trot period.

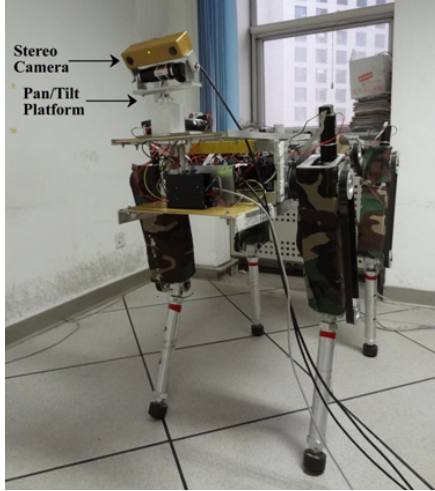


Fig. 5 Experiments are performed on the FROG quadruped robot, built at our lab. The stereo camera is installed on the Pan/Tilt platform for terrain perception.

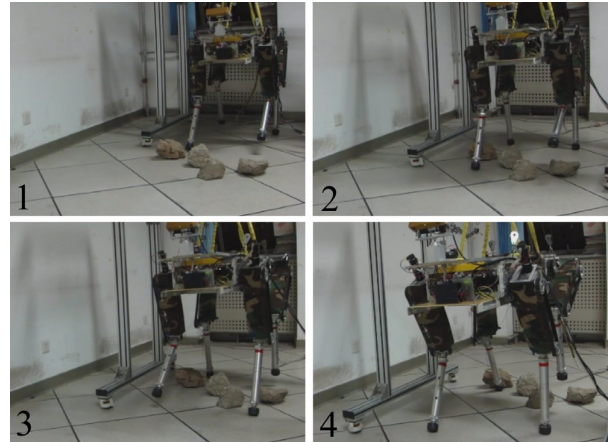
B. Evaluations and Discussions

Fig. 7 shows the foot trajectories in vertical direction while crossing over the complicated terrains. To display the foot trajectories intuitively, the positions are computed in the coordinate systems fixed at hip joints. Some explanations and analysis are given as follows,

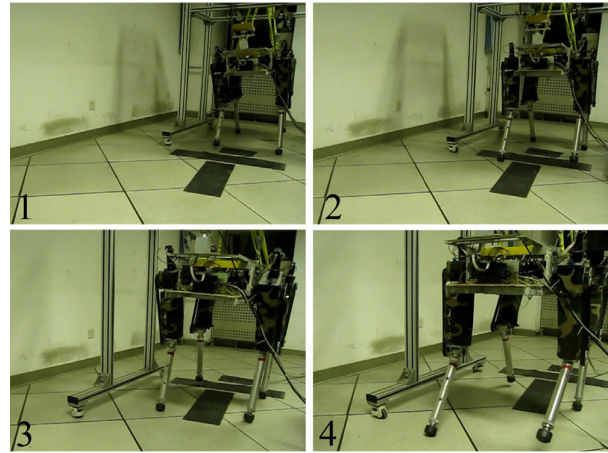
(1) In the three experiments, as indicated by the periods of Trot1 to Trot3 and Walk1 to Walk3, the quadruped robot crosswise selects trot gait and walk gait based on terrain conditions. When any of the legs move in the local area which is not even or contains forbidden areas, the robot employs walk gait to reduce the locomotion speed and ensure the stability. When the four legs have free spaces for choosing footholds, the robot switches to trot gait to increase the locomotion speed. Trot1 and Trot3 periods in each experiment denote the trotting on flat ground areas before and after crossing over the complicated terrains, and Trot2 describes the trotting while the complicated terrains locating between the front and hind legs.

(2) As described by the Walk1 to Walk4 periods in Fig. 11(a) and the Walk1 and Walk3 periods in Fig. 7(c), the quadruped robot detects the convex obstacles. To avoid the collision, the robot increases the vertical height while crossing. For example, in experiment 1, the feet are lifted up 0.15m more compared to normal locomotion for safety.

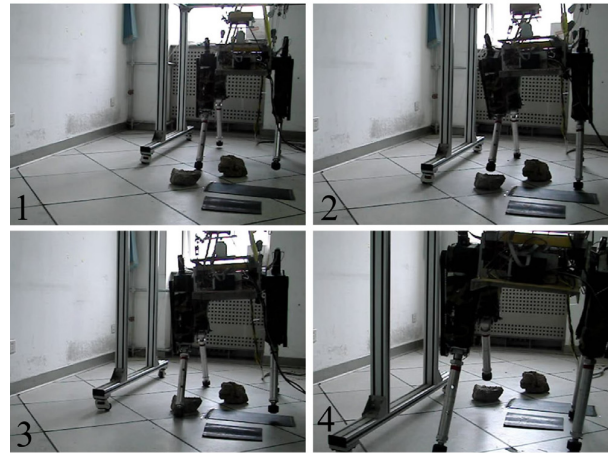
(3) In Fig. 7(b), the front legs and the hind legs cross over the forbidden areas in Walk1 and Walk2, and in Fig. 7(c), the left legs cross over the forbidden areas in Walk1 and Walk3.



(a) Locomotion on Convex Obstacle Terrain



(b) Locomotion on Forbidden Area Terrain



(c) Locomotion on Terrain with Convex Obstacles and Forbidden Areas

Fig. 6 Snapshots of adaptive locomotion in the three experiments. (a) and (b) show the locomotion on convex obstacle terrain and forbidden area terrain separately, (c) displays the locomotion on terrain with convex obstacles and forbidden areas. Numbers from 1 to 4 indicate the motion sequence in each experiment.

To reduce time and energy consumption, the quadruped robot adjusts the walk gait with relatively lower vertical height. For example, in experiment 2, the heights are reduced about 0.05m.

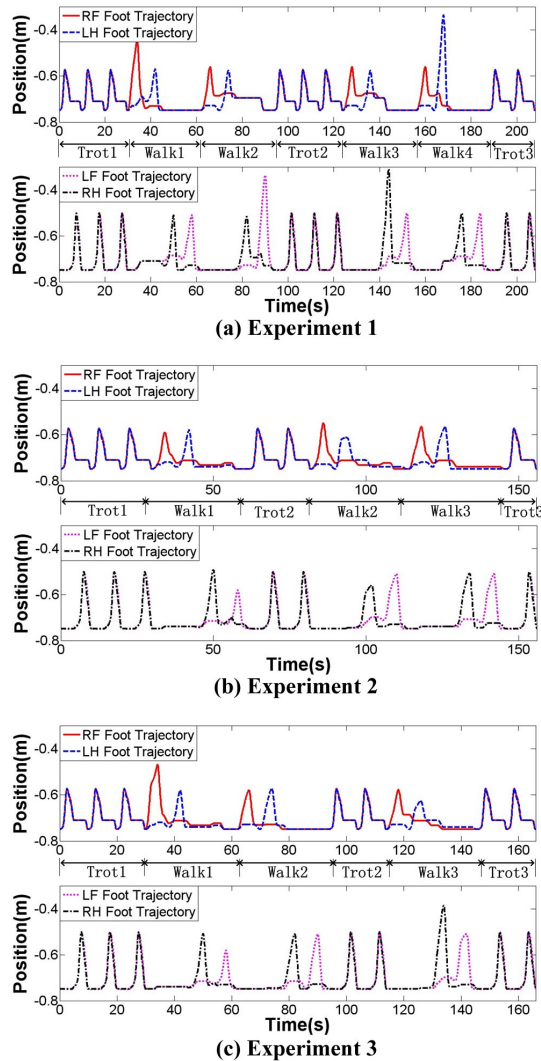


Fig. 7 Foot trajectories along vertical line while crossing over the perception terrains. (a) Experiment 1 over convex obstacle terrain, (b) Experiment 2 over forbidden area terrain, (c) Experiment 3 over complex terrain. For each subgraph, red solid curve and blue dashed curve stand for RF foot trajectory and LH foot trajectory, and pink dotted curve and black dashdotted curve stand for LF foot trajectory and RH foot trajectory. Walk1, Walk2 and Walk3 indicate walk periods, Trot1, Trot2 and Trot3 denote trot periods.

To verify the effectiveness of the proposed motion planning methods while convex obstacles and forbidden areas crossing, motor currents are sampled as in Fig. 8. Taking knee joints of the quadruped robot for example, RF knee's currents during convex obstacle jumping and forbidden area overstriding in experiment one and experiment two are compared in the top subgraph. Similarly, for the complex terrain in experiment

three, RF knee's currents and LF knee's currents are displayed in the bottom subgraph. The crossing period in Fig. 8 can be classified into the anterior and the posterior segments. In the front part, the current values for forbidden area overstriding are almost smaller compared to the values for convex obstacle jumping on the negative half axis. However, in the rear part, the situation is reverse on the positive half axis. This is in consistent with the principle of time and energy consumption. For convex obstacle jumping, the knee joint should overcome the gravity to lift up the shank to a certain height at the beginning, and the short arm of the gravity contributes to the shank's dropping at the ending. For forbidden area overstriding, the shank is mainly moved forward at a low height. Less energy is needed to overcome the gravity at the beginning. As the angle between the shank and the ground level decreases, the arm of the gravity increases. Therefore, larger holding torque is needed in the phase of the shank's dropping.

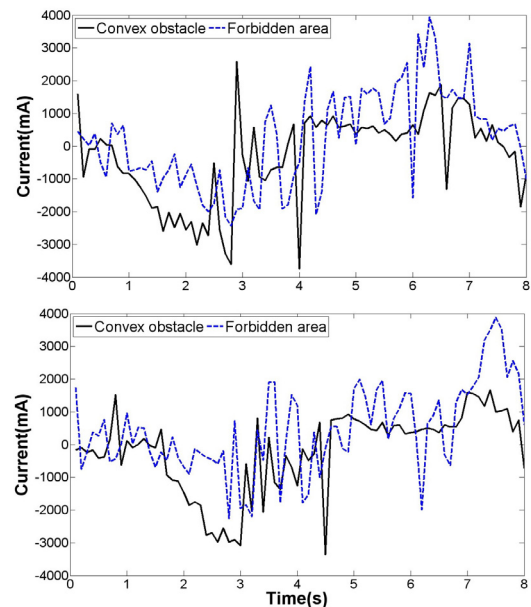


Fig. 8 (top) Black solid curve is RF knee's motor current trajectory in experiment 1 during convex obstacle jumping, blue dashed curve is RF knee's motor current trajectory in experiment 2 during forbidden area overstriding. (bottom) Black solid curve and blue dashed curve stand for RF knee's motor current trajectory during convex obstacle jumping and LF knee's motor current trajectory during forbidden area overstriding in experiment 3.

One point in the locomotion that needs to be noticed is the slippage factor, especially at the moments of crossing with larger moving steps. In order to generating larger step, the legs should bend heavily compared to normal state. This would not only increase tangential force but also decrease maximum static friction force between the foot and supporting surface. When the tangential force is greater than the maximum static friction force, slippage would happen inevitably. An effective measure to solve the problem is to replace the material fixed at the end of the foot with others which have larger friction coefficients.

IV. CONCLUSIONS AND FUTURE WORK

In this paper, we proposed a motion planning algorithm with the compliant control method for quadruped adaptive locomotion in ground plane scattered with convex obstacles and forbidden areas based on on-board stereo vision. The experiment results on FROG quadruped robot prove the feasibility and validity and give some suggestions for quadruped locomotion.

The particularly significant element is the motion planning algorithm, used for programming the footholds for adaptive locomotion. To find the rational waypoints for crossing over convex obstacles and forbidden areas, the motion planning algorithm considers multiple gaits generation and gait transition to improve the moving performance. The quadruped robot crosswise selects trot gait and walk gait flexibly to get high locomotion speed and stability. This movement is in accord with natural quadruped animal locomotion to some extent.

The control architecture employs the compliant control method for the low level control. Considering the expandability of joints and the brevity of the iterative calculation, we use the data structure in which each node has one child and one sister. The forward kinematics model is built based on Rodrigues rotation formula and the numerical solution is applied into the inverse kinematics problem. According to the quadruped's stance phase and swing phase, the couple influences between different legs and the transition during phrase switching are seriously handled in the couple inverse dynamics model for the compliant control. The analyses of foot trajectories and motor currents demonstrate the reasonableness of motion planning towards different kinds of obstacles.

Future work will focus on the autonomous locomotion in outdoor environments. Furthermore, attentions should be paid to deal with the dynamic environments, such as ground planes with moving obstacles. These are of great benefits to practical applications for quadruped robots.

REFERENCES

- [1] K. Kato and S. Hirose, "Development of the quadruped walking robot, TITAN-IX — mechanical design concept and application for the humanitarian de-mining robot," *Adv. Robot.*, vol. 15, no. 2, 2001, pp. 191-204.
- [2] R. Hodoshima, Y. Fukumura, H. Amano and S. Hirose, "Development of track-changeable quadruped walking robot TITAN X-Design of leg driving mechanism and basic experiment," *Proceedings of the IEEE/RSJ International Conference on Intelligent Robots and Systems*, Taipei, Taiwan, 2010, pp. 3340-3345.
- [3] Y. Fukuoka, H. Kimura and A. H. Cohen, "Adaptive dynamic walking of a quadruped robot on irregular terrain based on biological concepts," *Int. J. Robot. Res.*, vol. 22, no. 3-4, 2003, pp. 187-202.
- [4] H. Kimura, Y. Fukuoka and A. H. Cohen, "Adaptive dynamic walking of a quadruped robot on natural ground based on biological concepts," *Int. J. Robot. Res.*, vol. 26, no. 5, 2007, pp. 475-490.
- [5] C. Maufroy, H. Kimura and K. Takase, "Integration of posture and rhythmic motion controls in quadrupedal dynamic walking using phase modulations based on leg loading/unloading," *Auton. Robot.*, vol. 28, no. 3, 2010, pp. 331-353.
- [6] C. Maufroy, H. Kimura and T. Nishikawa, "Stable dynamic walking of the quadruped "Kotetsu" using phase modulations based on leg loading/unloading against lateral perturbations," *Proceedings of the IEEE International Conference on Robotics and Automation*, Saint Paul, Minnesota, 2012, pp. 1883-1888.
- [7] I. Poulakakis, J. A. Smith and M. Buehler, "Modeling and experiments of untethered quadrupedal running with a bounding gait: the Scout II robot," *Int. J. Robot. Res.*, vol. 24, no. 4, 2005, pp. 239-256.
- [8] J. Estremera and P. G. de Santos, "Generating continuous free crab gaits for quadruped robot on irregular terrain," *IEEE Trans. Robot.*, vol. 21, no. 6, 2005, pp. 1067-1076.
- [9] M. Raibert, K. Blankespoor, G. Nelson and R. Playter, "BigDog, the rough-terrain quadruped robot," *Proceedings of the 17th World Congress on the International Federation of Automatic Control*, Seoul, Korea, 2008, pp. 10823-10825.
- [10] M. Raibert, *Legged Robots that Balance*. MIT Press, Cambridge MA, 1986.
- [11] M. Raibert, "Trotting, pacing, and bounding by a quadruped robot," *J. Biomech.*, vol. 23, Suppl.1, 1990, pp. 79-81, 83-98.
- [12] Xuesong Shao, Yiping Yang and Wei Wang, "Obstacle crossing with stereo vision for a quadruped robot," *Proceedings of the IEEE International Conference on Mechatronics and Automation*, Chengdu, China, 2012, pp. 1738-1743.
- [13] Xuesong Shao, Yiping Yang, and Wei Wang, "Trajectory planning and posture adjustment of a quadruped robot for obstacle striding," *Proceedings of the IEEE International Conference on Robotics and Biomimetics*, Phuket, Thailand, 2011, pp. 1924-1929.
- [14] S. Kajita, H. Hirukawa, K. Yokio and K. Harada, *Humanoid Robots*. Tsinghua University Press, Beijing, China, 2008.
- [15] Bin Li, *The Algorithm and Implementation of Gait Control and Gait Transition for Quadruped Robots*. Ph.D. thesis, Institute of Automation, Chinese Academy of Sciences, Beijing, China, 2010.
- [16] C. A. Balafoutis, "A survey of efficient computational methods for manipulator inverse dynamics," *J. Intell. Robot. Syst.*, vol. 9, no. 1-2, 1994, pp. 45-71.
- [17] E. Carrera and M. A. Serna, "Inverse dynamics of flexible robots," *Math. Comput. Simulat.*, vol. 41, no. 5-6, 1996, pp. 485-508.
- [18] R. Featherstone and D. Orin, "Robot dynamics: equations and algorithms," *Proceedings of the IEEE International Conference on Robotics and Automation*, San Francisco, CA, 2000, pp. 826-834.
- [19] R. Featherstone, *Rigid Body Dynamics Algorithms*. Springer Science+Business Media, LLC, New York, USA, 2008.
- [20] M. Kalakrishnan, J. Buchli, P. Pastor, M. Mistry, and S. Schaal, "Learning, planning, and control for quadruped locomotion over challenging terrain," *The International Journal of Robotics Research*, vol. 30, no. 2, 2011, pp. 236-258.
- [21] Xuesong Shao, Yiping Yang and Wei Wang, "Ground substrates classification and adaptive walking through interaction dynamics for legged robots," *J. Harb. Inst. Technol.*, vol. 19, no. 2, 2012, pp. 100-108.
- [22] Wei Wang and Yiping Yang, "Turning maneuvers and mediolateral reaction forces in a quadruped robot," *Proceedings of the IEEE International Conference on Robotics and Biomimetics*, Phuket, Thailand, 2011, pp. 515-520.